MINIMIZING BLADE-FLUID ENERGY LOSSES IN CENTRIFUGAL HYDRAULIC PUMP IMPELLERS

Viorel BOSTAN, Andrei PETCO

Abstract: *This paper examines the reduction of energy losses in the blade-fluid interaction by applying the methods of computational fluid dynamics in combination with the heuristic optimization methods, specifically the evolutionary algorithm based on the criterion of increasing the mechanical efficiency with the restriction of maintaining the pumping height of the fluid. The methods presented in the work were applied under the condition of maintaining the continuity of the curve line of the profile on the entire length of the blade included between its leading and trailing edge. The solutions used to create the profile of the blades were exposed, which led to the reduction of the energy losses in the blade-fluid interaction, to the increase of the hydraulic efficiency of the impeller from 56% to 61% and to the increase of the pump's mechanical efficiency by 3.2%.*

Key words: *centrifugal hydraulic pump; pump impeller; profiled blades; energy losses; Computational Fluid Dynamics (CFD).*

1. INTRODUCTION

Currently, centrifugal pumps, used in various branches of industry, are some of the most widespread types of pumps. Centrifugal pumps produced in the Republic of Moldova are used in the chemical, petroleum, atomic, pharmaceutical, food, etc. industries. Hence, the problem of optimizing the parts of centrifugal pumps is a current one and it is of great interest to the Moldovan industry [1].

This paper presents the optimization procedure of the CH-6,3-20-1,1-2 centrifugal pump impeller, made using the ANSYS optiSLang software, in conjunction with ANSYS CFX used as a solver, for modeling the fluid flow in the area of pump flow and receiving the characteristics of modified impellers.

We can see that the optimization is an iterative process (fig. 1), therefore applying the most favorable simulation settings to improve the centrifugal pump impeller optimization process is crucial to create an effective optimization process.
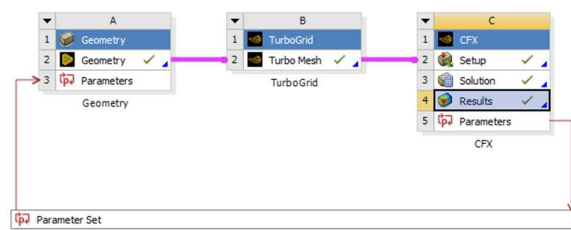

Fig.1. Optimization process produced in ANSYS Workbench

As optimization parameters, the authors chose to determine the shape of the impeller blades and the number of blades. As for optimization criteria, the emphasis was put on the minimization of the impeller torque, while maintaining the head of the impeller.

The impeller torque reduction was chosen as an optimization criterion because, based on equation 1, the efficiency of the impeller is inversely proportional to the input torque, if the pump head, flow rate and impeller angular velocity remain constant.

$$\eta_h = \frac{\rho g H Q}{\omega N} \tag{1}$$

where: ρ is the density, H – pump head, Q – flow rate ω is impeller angular velocity and N – impeller.

It should be noted that when calculating the overall efficiency of the pump, the mechanical and volumetric efficiency of the hydraulic part of the pump was not taken into account; for this type of pump, their influence degree on the efficiency is not high, will not change considerably with the optimized impeller and will be approximately equal to both the initial impeller and the optimized impeller.

2. GEOMETRIC MODEL

The ANSYS DesignModeler module was used to obtain the geometric model. The initial geometry represents the geometric model of the impeller of the CH-6,3-20-1,1-2 canned motor centrifugal pump. Only the geometry of the blade was subjected to parameterization, the hub and shroud surfaces remaining unchanged. ANSYS BladeEditor tools were applied to obtain the parameterized geometric model. The parameterization scheme is presented in fig. 2.

Blade geometry was parameterized varying the β blade angle in 5 points, keeping the blade thickness distribution constant along the entire length of the camberline, identical to the original impeller.

The parameterization of the pump impeller was carried out in accordance with the scheme shown in fig.1. We can observe that the blades executed with a curvilinear working surface in the cross-section and placed with an angular pitch α on its outer diameter, have variable curvature between their leading edge n1 and trailing n5, inscribed at an angle θ and are located on the inner diameters d and outer D, respectively.

The blades have the geometric shape represented by the camberline, which passes through the points n1...n5 with the entrance edge defined by the point n1 expressed by the inner diameter D and the blade angle $\beta1$, for the points n2...n4 characterized, respectively, by the angular coordinates $\Delta\theta2$, $\Delta\theta3$ and $\Delta\theta4$ and, respectively, by the blade angles $\beta2$, $\beta3$, $\beta4$, and for the exit edge of the curvature line in point n5 expressed by the angular coordinate $\Delta\theta5$, the

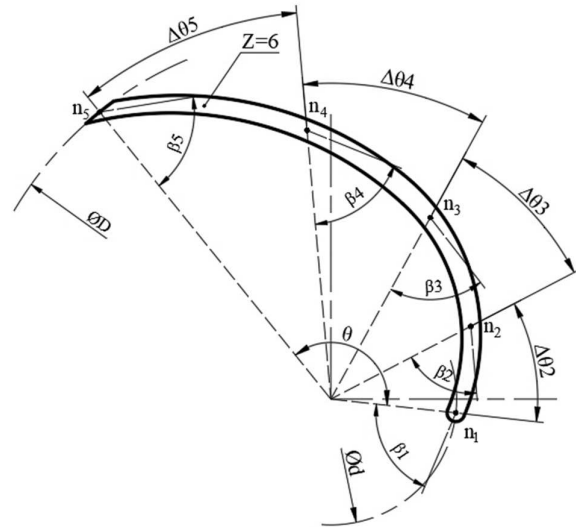angle of the blade $\beta5$ and the outer diameter of the rotor D.

Fig.2. Parametrization impeller geometry scheme

After parameterization, the geometric model shown in figure 3 is formed. The geometric model was made for a single blade, to minimize the necessary computing resources.
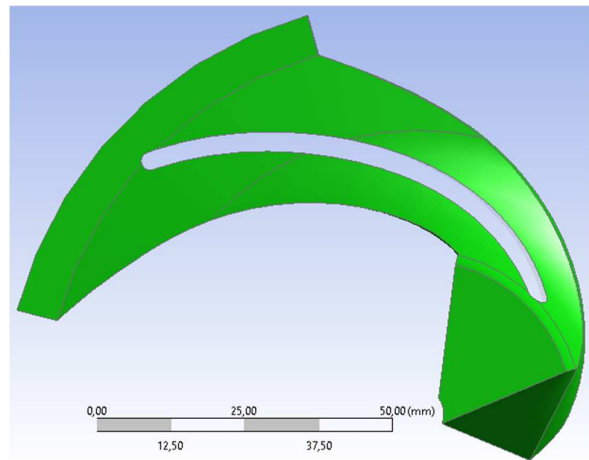

Fig.3. Initial geometric model

3. DISCRETIZATION PROCESS

The discretization was done in ANSYS TurboGrid, a powerful meshing tool specifically designed for turbomachinery applications (turbines, pumps, and compressors). ANSYS TurboGrid was chosen because it provides automated meshing algorithms that can generate a mesh with complex blade geometries, consisting of inducers, impellers, vanes, etc.,

without the intervention of an engineer. Mesh autonomy is one of the key factors in creating a multi-iteration optimization process.

Figure 4 shows a grid created in ANSYS TurboGrid. The desired achievable parameter y+, equal to 1, was used as the grid parameters, with the accepted Reynolds number of fluid flow in the impeller equal to 5×10^5.
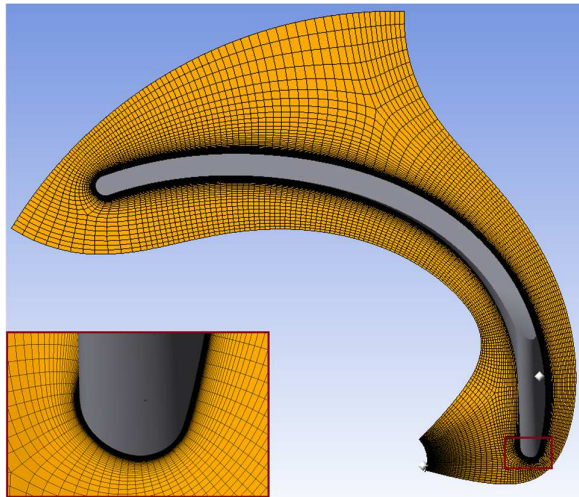

Fig.4. Discretization model

This should make it possible to obtain a sufficiently dense structured grid, including in the boundary layer, which is necessary for an adequate description of the fluid flow.

4. ESTABLISHING INITIAL AND BOUNDARY CONDITIONS

A number of initial conditions were applied in the study (fig.5).

At the inlet to the flow section, the total pressure is indicated (stable), $P_{inlet} = 10^6 \ Pa$, the flow direction is normal. It is assumed that at the entrance to the system the flow consists entirely of water in liquid form, with low turbulence (1%).

At the outlet, the flow rate is indicated for the nominal flow rate $Q_{outlet} = 1,75 \ (kg/s) \ / \ n$, where n is the number of impeller blades. At the outlet of the system, the flow characteristics associated with turbulence and cavitation are calculated by the solver (Zero Gradient).

The impeller area rotates at *2950 min-1*, at zero reference pressure (Pref = 0 atm).

The flow is isothermal, at a temperature of 25°C.

In the initial state, the liquid in the design zone consists entirely of water in liquid form.

Wall type boundary conditions are applied to walls with a "no slip" specification - the velocity on these surfaces is assumed to be zero, which makes it easier to model the flow in the area near the wall.

The model does not take into account the gravitational forces and the roughness of contact surfaces.

The simulation is based on a two-phase continuous fluid model consisting of:
• water in liquid form at 25°C;
• water vapor at 25°C.

Rotational *Periodic Interface* was applied to the edge surfaces of the domain, due to the fact that only one blade was taken as the calculation domain.

As the timeline control model, the Physical Timeline option was selected. Since the main movement under study is the rotational movement of the impeller at a constant speed, when searching for the optimal step, it should be tied to the angular velocity.[2] The optimal time step was equal to $1/\omega = 0.0032$ s. Reducing the step below this level does not bring tangible results.
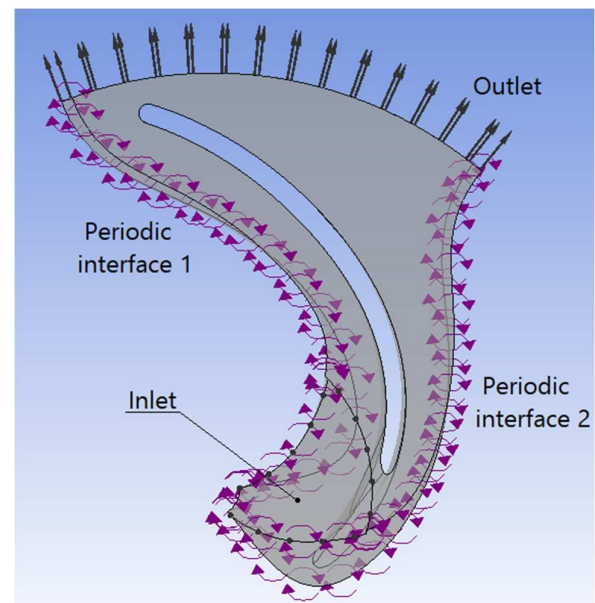

Fig. 5. Applying initial and boundary conditions in ANSYS CFX

Frozen rotor was chosen as the interface between domains (Interface model), which

better models interaction between different domains, compared to the Stage model (mixing plane), which only mediates the velocities on the interface surface.

Due to the limited computational resources, the simulation uses the Steady-State calculation. This approach to modeling of turbulent flow differs in that the flow field is averaged over time.

5. ESTABLISHING THE MATHEMATICAL MODEL

An important step for describing the fluid flow inside the pump to obtain realistic numerical results is to establish the mathematical model of turbulence and cavitation.

One of the main problems in calculating the fluid flow consists in the simulation of the turbulence process that consists of expressive fluctuations in the flow field in time and space, which can have a significant effect on the flow image. Turbulence occurs when the inertial forces in the fluid become significant compared to the viscous forces and is characterized by a Reynolds number reaching the order of 10^6. [3] It is a complex process, which cannot be solved by direct calculation of Navier-Stockes equations.

Taking into account that Steady-State was used in the study, a turbulence model based on the *RANS (Reynolds-averaged Navier–Stokes)* equations was selected, because it uses the statistical averaging procedure to obtain equations, which considerably reduce the computational resources spent.

In the given research, the *SST (Menter's Shear Stress Transport)* turbulence model, eq. (2) and (3), is used [4]:

$$\frac{\partial(\rho k)}{\partial t} + \frac{\partial(\rho u_j k)}{\partial x_j} = P - \beta^* \rho \omega k +$$

$$+ \frac{\partial(\rho k)}{\partial x_j}\left[(\mu + \sigma_k \mu_t)\frac{\partial k}{\partial x_j}\right] \qquad (2)$$

$$\frac{\partial(\rho \omega)}{\partial t} + \frac{\partial(\rho u_j \omega)}{\partial x_j} = \frac{\gamma}{v_t}P - \beta \rho \omega^2 +$$

$$+ \frac{\partial}{\partial x_j}\left[(\mu + \sigma_\omega \mu_t)\frac{\partial \omega}{\partial x_j}\right] + 2(1 - F_1)\frac{\rho \sigma_{\omega 2}}{\omega}\frac{\partial k}{\partial x_j}\frac{\partial \omega}{\partial x_j} \quad (3)$$

where: $P = \tau_{ij}\frac{\partial u_i}{\partial x_j}$, ρ is the density and μ is the dynamic viscosity.

The advantage of the SST model over the above models consists its high accuracy of flows with unfavorable pressure gradients and separation, [5] which allows improved predictions of the turbulent shear stress in regions with high shear and adverse pressure gradients [6], as it simultaneously combines strengths of the k-ω (boundary layer flow description) and k-ε (fluid free flow description) models. [7]

The mass transfer model represents the cavitation model and it is defined by the Rayleigh-Plesset equation, which governs the dynamics of a spherical bubble in an incompressible fluid.
The cavitation model used in ANSYS CFX is the Zwart, Gerber, and Belamri model based on the Rayleigh-Plesset equation [Ansys CFX Solver Theory Guide]:

$$\dot{S}_{lv} = \begin{cases} Fvap\dfrac{3r_{nuc}(1 - r_v)\rho_v}{R_B}\sqrt{\dfrac{2}{3}\dfrac{P_v - P}{\rho_l}}, & P < P_v \\[4mm] Fcond\dfrac{3r_v\rho_v}{R_B}\sqrt{\dfrac{2}{3}\dfrac{P - P_v}{\rho_l}}, & P > P_v \end{cases}$$

The model is based on the calculation of the multiphase mass transfer rate per unit volume $\dot{S}_{lv}$. Mass transfer per unit volume is calculated using the nucleation site volume fraction r_{nuc}. [8]

The chosen radius of the nucleation site R_B is $1 \cdot 10^{-6}$ m, and the vapor saturation pressure $P_v = 3170$ Pa.

5. PROCESSING AND POST PROCESSING SETTINGS

The minimum requirements were chosen to optimize computing resources, ensuring numerical convergence, with minimal execution time.

A finite number of calculation iterations of 200 was chosen, and the calculation is also completed when the root means square residual error tolerance of 10^{-5} is reached. In order to control the convergence, the following indicators were chosen: domain imbalance,

static pressure at the inlet and outlet, as well as torque relative to the rotation axis applied to the pump impeller.
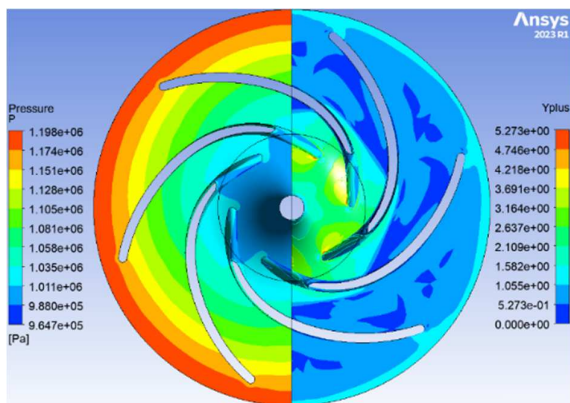

Fig.6. Representation of the pressure field and the distribution of the y+ parameter in ANSYS CFX post

After performing the calculation, the system displays the pressure at the outlet of the impeller and the moment of rotation of the impeller relative to the axis of rotation Z, as an indicator of the optimization criterion.

6. OPTIMIZATION PROCESS

The optimization process was based on the coupling of computational fluid dynamics and evolutionary algorithm methods. The application of these methods is necessary due to the complexity of the fluid flow process in the pump rotor, thanks to the pronounced turbulence phenomenon, which does not allow the description of the flow by analytically solving the Navier-Stokes equations and, respectively, the complexity of the multicriteria optimization process. Hence, this goal cannot be achieved using classical calculation and optimization methods.

The optimization process includes the following procedural actions:

1. Establishing a benchmark by performing flow simulation at initial geometric parameters of the pump rotor (fig.7). At the same time, due to this step, the numerical validation of the simulation results is performed because they can be compared with the results of the pump testing, carried out in accordance with the ISO 9906:1999 standard - Hydraulic performance acceptance tests.
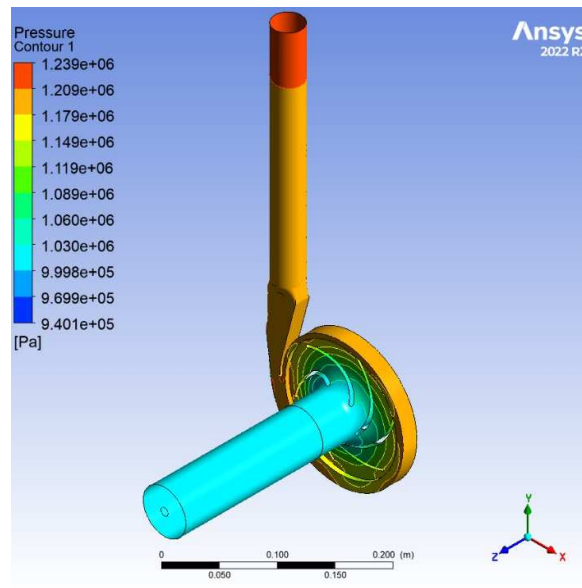

Fig.7. Results of numerical model validation

2. Choosing optimization parameters. As optimization parameters, 11 parameters describing the shape and number of blades were selected: blade angles $\beta1…\beta5$, angular coordinates $\Delta\theta2…\Delta\theta5$, inner diameter d and outer diameter of the impeller D, as well as the number of blades Z. In the figure 8, the θ angles are represented by parameter M, which represents the linear position of points n2...n5 on the curve.

3. Establishing optimization criteria. Increased efficiency was selected as optimization criterion, with the restriction of keeping the pumping head of the pump constant.

4. Setting up the limits to vary the parameters. The limits to vary the parameters are also shown in table 1.

Table 1

Establishing optimization parameters limits of the geometric model.

Inner diameter d, mm		Outer diameter D, mm	Blade angles $\beta1...\beta5$, °
17 ÷ 28		110 ÷ 138	50 ÷ 80
M_2, %	M_3, %	M_4, %	No. of blades z
25±12,5	50±12,5	75±12,5	3 ÷ 8

The sampling of parameters between the established limits was performed by means of the Latin Hypercube method. This step is necessary to obtain random combinations of parameter values. Totally 1200 design points
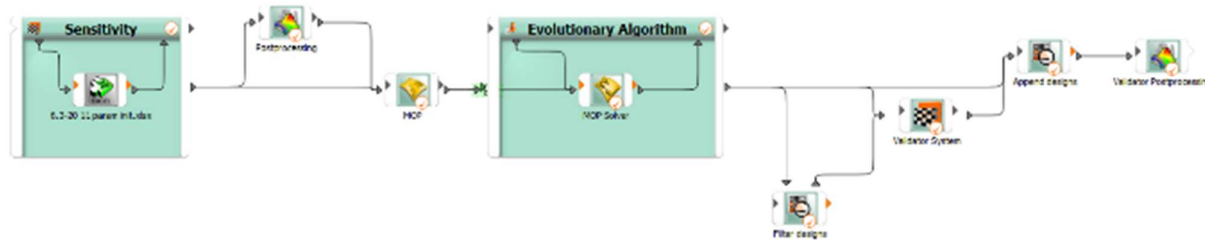
Fig.8. Optimization process produced in ANSYS optiSLang

were received, 200 for each of the number of blades (z = 3÷8). As a result of parameterization, based on these combinations of parameters, 974 successful geometries were created, which enabled to carry out the optimization process.

5. Carrying out a series of simulations based on the geometric models obtained from data received after sampling. Receiving a dataset that has been loaded into ANSYS optiSLang (fig.8).

6. Applying linear regression and Kriging method to the dataset received from the series of simulations to obtain a response surface.

A response surface is a mathematical model that describes the relationship between input variables (parameters) and a response variable (the optimization variable) of interest. Response surface is usually used to represent the behavior of a complex physical system. The application of the response surface is rational because the application of Direct Optimization in the given case is computationally expensive and because of a large number of input parameters, it does not converge.

Also, obtaining the correlation matrix helped to analyze the correlation between the variables in the dataset, which shows the pairwise correlations between the variables.

It was obtained, the Coefficient of Performance (COP) matrix (fig.9), which provides information about the influence of parameters on optimization criteria values.
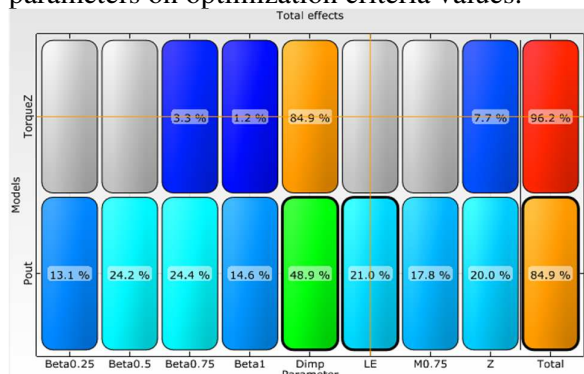

Fig.9. Coefficient of Performance (COP) matrix

Based on the COP matrix, we can identify the main parameters that affect the moment of rotation of the impeller, namely, the diameter of the impeller D and the number of blades z. The correlation, almost linear, of these parameters and the main optimization criterion is shown in the figure 10.
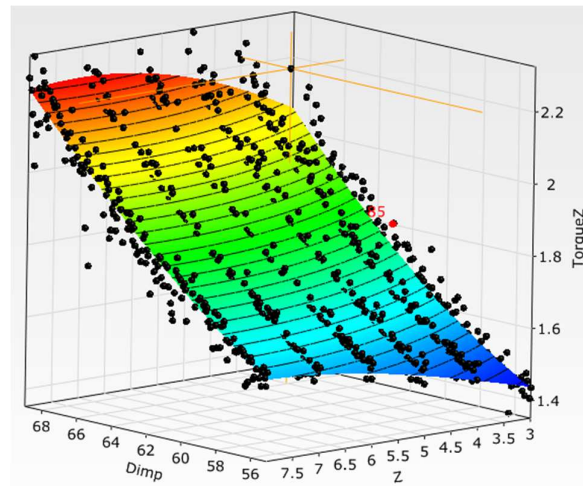

Fig.10. Influence of impeller diameter and number of blades on the moment of impeller rotation

6. Applying the evolutionary algorithm. Due to the fact that there is more than one objective function in the optimization process, the process is multicriterial. The mathematical apparatus necessary to set and solve such multicriteria or multicriteria problems is very extensive and represents a special branch of optimization theory [9]. As an optimization algorithm, an Evaluative Algorithm was proposed by optiSLang as the most suitable optimization algorithm.

The evolutionary algorithm, being a recursive process, consists of the following steps: creation of initial population, evaluation of decisions, application of genetic operators (in the given case of mutation), evaluation and selection of solutions [10]. The iterations are repeated until optimal pump rotor parameters are established.

The evolutionary algorithm has examined more than $2 \cdot 10^4$ samples, iterations have not yet converged. The geometry study is presented in the figure 11. It should be noted that the selected geometry on the margin is marked in red.
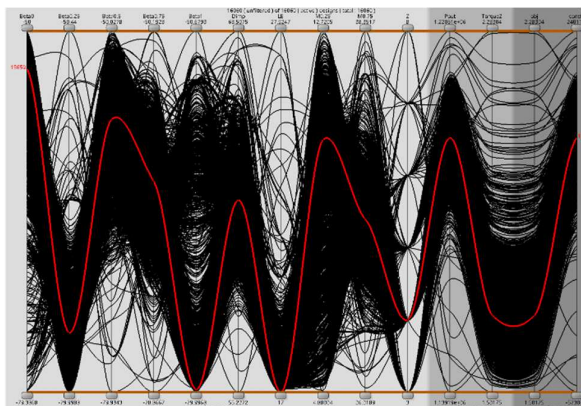

Fig.11. Geometries explored by the Evolutionary Algorithm using response surface data

7. Carrying out fluid flow simulations in the modified impeller of the pump and comparing the data with those obtained when simulating the flow in the rotor with initial geometric parameters fig.12.
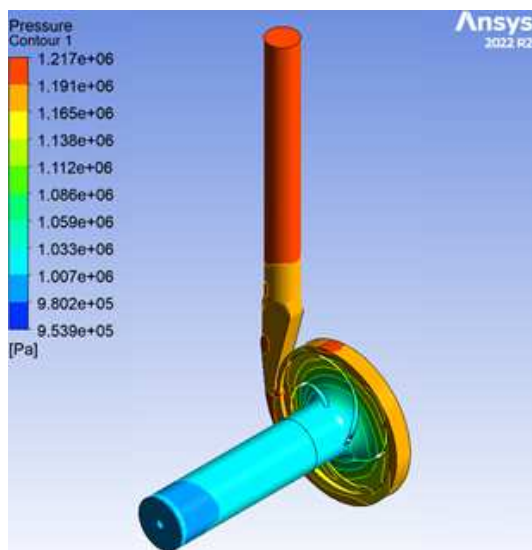

Fig.12. Simulation results of a pump with an optimized impeller

6. ANALYSIS OF THE OBTAINED RESULTS

As a result of optimization, the hydraulic efficiency of the pump has been significantly increased.

The comparison of the characteristics of the original and optimized impeller is presented in table 2.

There is a drop in pressure within the allowed limits of ± 5 % from BEP flowrate (Q_{nom} = 20 m³/h), but also an increase in rotor efficiency from 56% to 61%.

Table 2
Comparison of characteristics of the original and optimized pump.

	Head, m (H$_2$O)	Torque, Nm	Impeller efficiency	Pump efficiency
Original	20,8	2,03	0,56	0,363
Optimized	19,9	1,7764	0,61	0,396

The blade geometry of the optimized impeller is shown in figure 13.

It should be noted that as a result of the optimization process, the shape of the impeller blades has changed, but also the number of blades has decreased to 4.
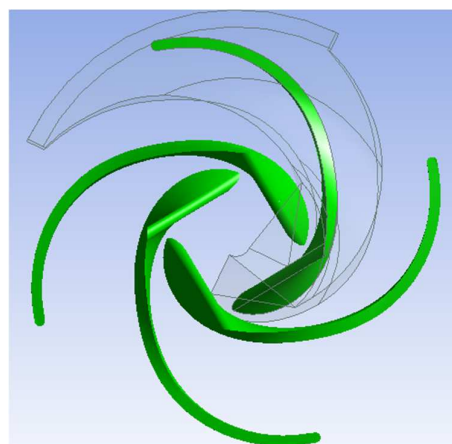

Fig.13. Optimized blade geometry

The comparison of the original and optimized profile is shown in figure 14. It can be seen that when changing the number of blades from 6 to 4, the θ angle increases significantly.
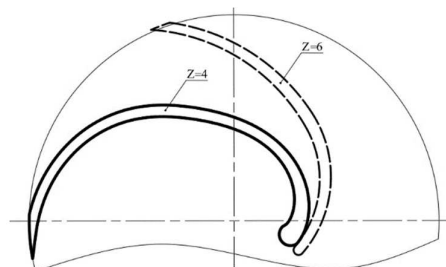

Fig.14. Comparison of the shape of the original and optimized blades (according to the projection hub)

7. CONCLUSIONS

Mechanical efficiency of centrifugal pumps mainly depends on the diameter of the impeller, and also on the number and geometric profile of blades. An optimization process was carried out based on the methods of computational fluid dynamics in combination with the heuristic optimization methods defined by the evolutionary algorithm based on the criterion of increasing the mechanical efficiency, with the restriction of maintaining the pumping height of the fluid. The application of the optimization process to create the blade profile led to the reduction of energy losses at the blade-fluid interaction and to the increase of the hydraulic efficiency of the rotor from 56% to 61%, while the mechanical efficiency of the pump increased by 3.2%.The optimized geometry is submitted for patenting. It should also be mentioned that the complete optimization of the rotor (with the surface of the hub and the shroud) is also to be carried out.

8. REFERENCES

[1] Petco, A. Dezvoltarea constructiv-funcțională a pompelor centrifuge prin optimizarea multiparametrică și simulările CFD. Presented at the CSMD 2019, 26-29 martie, 2019, Chișinău (2019)

[2] Petco, A. Simularea numerică a curgerii lichidului în organele de lucru a pompei centrifuge prin intermediul Ansys CFX. Presented at the CSMD 2021, 23-25 martie, 2021, Chișinău (2021)

[3] Gülich J.F. Centrifugal Pumps. Springer International Publishing, Cham (2020)

[4] Menter, F.R. Two-equation eddy-viscosity turbulence models for engineering applications (1995), AIAAJournal, doi/10.2514/3.12149

[5] Menter, F.R., Sechner, R., Matyushenko, A. Best Practice: RANS Turbulence Modeling in Ansys CFD (2022)

[6] Ansys CFX Solver Theory Guide. Release 2021 R2. ANSYS, Inc. (2021)

[7] Bostan, V. Modele matematice în inginerie: probleme de contact: modelări și simulări numerice în aero-hidrodinamică. s.n., Chișinău (2014), ISNB 9789975808316

[8] Zwart, P., Gerber, A.G., Belamri, T. A two-phase flow model for predicting cavitation dynamics. Fifth International Conference on Multiphase Flow. (2004)

[9] Principles of Optimal Design. Control systems and optimization. Cambridge (2017) ISBN: 9781107132672

[10] Slowik, A., Kwasnicka, H. Evolutionary algorithms and their applications to engineering problems. Neural Comput & Applic. 32, 12363–12379 (2020). https://doi.org/10.1007/s00521-020-04832-8

Minimizarea pierderilor energetice pală-fluid în rotoarele pompelor hidraulice centrifuge

În lucrare se examinează reducerea pierderilor energetice la interacțiunea pală-fluid, prin aplicarea metodelor dinamicii computaționale a fluidelor în combinație cu metodele euristice de optimizare definite prin algoritmul evolutiv bazat pe criteriul majorării randamentului mecanic, având ca restricție păstrarea înălțimii de pompare a fluidului. Metodele expuse în lucrare au fost aplicate cu condiția păstrării continuității liniei de curbură a profilului pe întreaga lungime a palei cuprinsă între muchia de intrare și de ieșire a acesteia. Sunt expuse soluțiile utilizate la crearea profilului palelor care au condus la reducerea pierderilor energetice, la interacțiunea pală-fluid și la majorarea randamentului hidraulic al rotorului de la 56% la 61%, în timp ce randamentului mecanic al pompei s-a majorat cu 3,2%.

Viorel BOSTAN, Dr. hab., Professor, Rector, Technical University of Moldova, National Centre of Space Technologies, Rep. Moldova, city Chisinau, 168 Stefan cel Mare Avenue, Rectorate, viorel.bostan@adm.utm.md

Andrei PETCO, Assistant Lecturer, Technical University of Moldova, Faculty of Mechanical and Industrial Engineering and Transport, Design Engineer, S.R.L. „CRIS", Rep. Moldova, city Chisinau, 9/8 Studentilor str., off. 6-214, andrei.petco@tcm.utm.md